RAA 2020 Vol. **20** No. **3**, 28(14pp) doi: 10.1088/1674–4527/20/3/28

http://www.raa-journal.org *http://iopscience.iop.org/raa*

***R**esearch in*
***A**stronomy and*
***A**strophysics*

Inference on disk-jet connection of MAXI J1836–194 from spectral analysis with the TCAF solution

Arghajit Jana, Dipak Debnath*, Sandip K. Chakrabarti and Debjit Chatterjee

Indian Centre for Space Physics, 43 Chalantika, Garia St. Rd., Kolkata, 700084, India; *dipakcsp@gmail.com*

Received 2019 April 10; accepted 2019 September 5

Abstract Galactic transient black hole candidate (BHC) MAXI J1836–194 was discovered on 2011 Aug 30, by MAXI/GSC and Swift/BAT. The source activity during this outburst continued for $\sim$ 3 months before entering into the quiescent state. It again became active in March 2012 and continued for another $\sim$ 2 months. In this paper, $3-25$ keV RXTE/PCA spectra from the 2011 outburst and $0.5-10.0$ keV Swift/XRT data during its 2012 outburst are analyzed with the two-component advective flow (TCAF) model based fits files in XSPEC. We calculate the X-ray contributions coming from jets/outflow using a newly developed method based on the deviation of the TCAF model normalization. We also study the correlation between observed radio and estimated jet X-ray fluxes. The correlation indices (b) are found to be 1.79 and 0.61, when the 7.45 GHz Very Large Array (VLA) radio flux is correlated with the total X-ray and jet X-ray fluxes in $3-25$ keV range respectively. It has been found that the jet contributes in X-rays up to a maximum of 86% during its 2011 outburst. This makes the BHC MAXI J1836–194 strongly jet dominated during the initial rising phase.

Key words: X-Rays: binaries — stars individual: (MAXI J1836–194) — stars: black holes — accretion, accretion disks — ISM: jets and outflows — radiation: dynamics

1 INTRODUCTION

Jets and outflows are very common in active galactic nuclei (AGNs). They are also observed in many Galactic black hole candidates (BHCs), such as GRS 1758–258 (Rodríguez et al. 1992), 1E 1740.7–2942 (Mirabel et al. 1992) and Cyg X-1 (Stirling et al. 2001). In general, two types of jets are identified in Galactic BHCs: continuous or compact jets and discrete or blobby jets (see, Chakrabarti & Nandi 2000 for more details). The exact mechanism for the production of jets is still unclear. In the literature, several models have been put forward to explain jets and outflows (Blandford & Znajek 1977; Blandford & Payne 1982; Chakrabarti & Bhaskaran 1992). In general, the magnetic field is considered to be the reason behind the collimation and acceleration of jets (Camenzind 1989).

It is well established that the accretion disk and jets are connected. This has been observed in many black hole (BH) sources. Traditionally, radio emission is considered to be originated from the jet while the X-ray is originated from the accretion disk. Thus, observation of radio/X-ray correlation indicates a coupling between the accretion disk and the jet (Hannikainen et al. 1998; Corbel et al. 2000, 2003). Also, it is observed that the outflow flux depends on the spectral state evolution (Fender et al. 2004). Several theoretical works have been put forward to explain the coupling between the accretion disk and jet (Falcke & Biermann 1995; Heinz & Sunyaev 2003). Several self-consistent works have been carried out on the disk-jet connection based on the transonic flow model (Chakrabarti 1999a,b; Chattopadhyay & Das 2007; Aktar et al. 2015).

Chakrabarti (1999a,b) (hereafter C99a and C99b respectively) and Das & Chakrabarti (1999) have calculated the outflow rate from the inflow accretion rate using hydrodynamics of in-falling and outgoing transonic flows. They show that the thermal pressure could be sufficient to supply matter to the outflows and accelerate them from low to moderate Lorentz factors (Chattopadhyay & Chakrabarti 2001, 2002). Transonic flow solutions naturally connect the disk and jet because in the presence of a shock, entropy rises and the post-shock region becomes the source of the outflow branch (see fig. 2 of Das & Chakrabarti 1999). So, they belong to the same class of solutions with opposite boundary conditions in the sense that an accretion flow is subsonic at infinity and supersonic at the BH horizon while

* Corresponding author

the jet is subsonic close to the horizon and supersonic at infinity (Chakrabarti 1989). The terminal velocity of an outflow is similar to the sound speed ($a \sim \sqrt{T}$) at the sonic point (Chattopadhyay & Chakrabarti 2000), so, the closer to the BH the sonic point is, the higher the thermal energy is, and higher the terminal velocity is (which is clearly an effect of the thermal pressure). Of course, the presence of rotational energy or magnetic energy would increase the terminal velocity. The physics of the outflow is clear from the Bernoulli constant or the specific energy of the transonic flow (Chakrabarti 1989).

Using the properties of transonic flows, the two-component advective flow (TCAF) solution (Chakrabarti & Titarchuk 1995, hereafter CT95; Chakrabarti 1997 and references therein) for the accretion flow around a BH was proposed. This is a generalized transonic flow solution of radiative transfer equations considering both heating and cooling effects. In this solution, an accretion disk has two components of the inflowing matter: a low viscous, low angular momentum sub-Keplerian halo component surrounding a highly viscous, high angular momentum Keplerian disk component. It has been shown that there exists a critical viscosity parameter ($\alpha_{\rm cr}$) for viscous flow (Chakrabarti 1990b, 1996; Chakrabarti & Das 2004). The flow with super-critical value ($\alpha > \alpha_{\rm cr}$) makes a Keplerian disk while the flow with sub-critical value ($\alpha < \alpha_{\rm cr}$) composes a sub-Keplerian halo (CT95, Chakrabarti & Molteni 1995). The sub-Keplerian flow forms an axisymmetric shock at the centrifugal barrier and the inflowing matter slows down at the shock location (X_s) making the region hot and puffed-up. This post-shock region is known as the CENBOL or CENtrifugal pressure supported BOundary Layer. It acts as the so-called 'corona' or 'Compton cloud' (Sunyaev & Titarchuk 1980, 1985). Low energy photons coming from the Keplerian disk are inverse-Comptonized at CENBOL and become hard photons. They create the power-law (PL) component of the observed spectrum of BHs. The observed multi-color blackbody, i.e., disk blackbody (DBB) component, is due to thermal photons originating from the Keplerian disk (similar to a truncated Shakura & Sunyaev 1973 or SS73 disk, but the temperature distribution is modified by reflected hard photons).

In the TCAF solution, the CENBOL is also the base of the jet (C99a,b). Mass outflow rate depends on the accretion rate, shock radius and shock compression ratio (R), which is the ratio between post- and pre-shock densities. Matters are driven outward due to thermal pressure gradient force. The outflowing matter or jet moves slowly up to the sonic surface ($\sim 2.5X_s$, C99a,b). After that, they move away supersonically. Due to the adiabatic expansion, temperature falls as the jet moves away. It emits electromagnetic radiation in all wavebands. The theoretical dependence of the ratio of outflow and inflow rates on the compression ratio suggests that the outflow rate is not maximum in the hard state. Rather, it is maximum in the intermediate states when the shock strength is intermediate (C99a,b). In the intermediate states, matter supply from the companion is much higher than that in the hard state. As the Keplerian rate is increased, the CENBOL is cooled down and its size is reduced. When the jet base is cooled, the flow suddenly becomes supersonic, separating it from the CENBOL to produce blobby jets (Chakrabarti 1999b; Das & Chakrabarti 1999). The reduction of the outflow rate on the Keplerian disk rate has been verified by numerical simulations (Garain et al. 2012). In the soft state (SS), the Keplerian rate becomes very high and completely cools down the CENBOL, quenching the jet altogether.

Recently, TCAF solution has been successfully implemented as an additive table model into HEASARC's spectral analysis software XSPEC (Arnaud 1996) to fit a BH spectrum (Debnath et al. 2014, 2015a). Using the TCAF model fitted spectral analysis, accretion dynamics of several BHs have been explained satisfactorily (Mondal et al. 2014, 2016; Debnath et al. 2015a,b, 2017; Chatterjee et al. 2016, 2019a; Jana et al. 2016, 2017; Bhattacharjee et al. 2017; Molla et al. 2017; Shang et al. 2019). To fit a BH spectrum with the TCAF model based fits file in XSPEC, one needs to supply two types of accretion rates (Keplerian $\dot{m}_d$, and sub-Keplerian $\dot{m}_h$) in units of Eddington rate, shock location (X_s) in Schwarzschild radius ($r_s = 2GM_{\rm BH}/c^2$) and shock compression ratio (R), if the mass ($M_{\rm BH}$ in $M_\odot$) and normalization are known. If the mass is unknown, one can also estimate it from the spectral analysis with the current version of the TCAF model fits file (Molla et al. 2016, 2017; Chatterjee et al. 2016; Jana et al. 2016, hereafter Paper-I; Debnath et al. 2017; Shang et al. 2019).

Unlike other models, TCAF model normalization N is constant across the spectral states for a particular BHC observed by a given instrument. Using this, Jana et al. (2017) (hereafter JCD17), separated the X-ray contribution from the accretion disk or inflowing matter ($F_{\rm inf}$) from jets or outflowing matter ($F_{\rm ouf}$). In JCD17, estimation of the jet X-ray flux ($F_{\rm ouf}$) and its properties during the 2005 outburst of the Galactic BHC Swift J1753.5–0127 are studied. In the current paper, using the same method, we separate X-ray contribution from jets/outflow for the Galactic BHC MAXI J1836–194 during its 2011 and 2012 outbursts. The properties of X-ray jets are also studied during the outbursts as well as the intervening quiescent phase.

Galactic transient BHC MAXI J1836–194 was discovered on 2011 Aug 29 by MAXI/GSC (Negoro et al. 2011). Swift/BAT also observed it simultaneously at R.A. $= 18^{\rm h}35^{\rm m}43^{\rm s}.43$, Dec $= -19^\circ19'12''.1$. During this out-

burst epoch, the source was active for ~ 3 months before going into the quiescent state. It again exhibited a short activity on March 2012 (Krimm et al. 2012; Yang et al. 2012a). This source was studied extensively in multiple wavebands: from radio and optical to X-rays (Ferrigno et al. 2012; Reis et al. 2012; Yang et al. 2012b; Russell et al. 2013, 2014a,b, 2015; Paper-I) during its 2011 outburst. It has a short orbital period of < 4.9 hr and a low inclination angle ($4^\circ - 15^\circ$; Russell et al. 2014a). This BHC is rapidly spinning with a spin parameter of $a = 0.88 \pm 0.03$ (Reis et al. 2012). Russell et al. (2014a) reported the mass of the BH to be $> 1.9\,M_\odot$, if the source is located at 4 kpc and $> 7\,M_\odot$, if the distance is 10 kpc. In Paper-I, employing TCAF model fitted spectra, Jana et al. suggested the mass of the BH to be in between $7.5 - 11\,M_\odot$ or, more precisely, $9.54^{+1.47}_{-2.03}\,M_\odot$. Russell et al. (2014a) also suggested that the binary companion could be a low mass ($< 0.65\,M_\odot$) star.

Our paper is organized in the following way: In Section 2, we briefly discuss our observation and data analysis methods or estimation of the jet X-ray fluxes. In Section 3, we examine results based on our analysis which includes the study of accretion flow properties of the source during its 2011 and 2012 outbursts, and the intervening quiescent phase. The evolution of the X-ray jet and its correlation with the observed radio flux density are discussed. Finally, in Section 4, we make concluding remarks.

2 OBSERVATION, DATA ANALYSIS AND METHOD OF ESTIMATING JET X-RAY FLUX

Jana et al. (2016) studied spectral and timing properties of MAXI J1836–194 during its 2011 outburst in details. Here, to estimate jet X-ray fluxes from the spectral analysis with the TCAF model, we employ $3 - 25$ keV RXTE Proportional Counter Unit 2 (PCU2) data of a total 35 observational IDs (starting from the first PCA observation day, i.e., 2011 August 31 or Modified Julian Day, i.e., MJD $= 55804$ till 2011 November 24 or MJD $= 55889$). For the data extraction and analysis, we follow the same method as in Paper-I. After spending ~ 4 months in the quiescent state, MAXI J1836–194 showed renewed activity in March 2012. We also analyzed ~ 15 Swift/XRT observations between 2012 March 12 and May 1. We apply the standard '$xrtpipeline$' command to extract $lighcurve$, $.pha$ and $.arf$ files. $0.5 - 10$ keV XRT spectra are fitted with the TCAF model. However, due to lack of data points with low signal-to-noise ratio, acceptable χ^2 statistics are obtained only for two observations during the 2012 outburst.

While fitting, a model normalization is used as a multiplicative 'factor' that converts the observed spectra to match the theoretical model spectra. In general, one may require different normalizations for different observations. In TCAF, however, the entire spectrum is an outcome of the solution and thus the model normalization 'N' only depends on the intrinsic source parameters, namely, the distance of the source and the disk inclination angle. Thus, it must remain a constant for a source observed by a particular satellite instrument. In our fit, one may still see some deviation of N, if the data are not of uniform quality, or if the disk precesses (i.e., if the effective disk area changes) or other physical processes such as X-rays from jets or outflows are present, which are not included in the current version of the theoretical model fits file. For instance, if a jet is present and the base contributes to the observed X-rays, we require a higher value of N while fitting the spectrum with the TCAF model fits file. This, together with a simultaneous observation of activities in radio, can confirm if the base of the jet is active in X-rays. While fitting the $3 - 25$ keV RXTE/PCA data of the 2011 outburst of MAXI J1836–194, we did not obtain a constant N value for all observations. The normalization N generally varied within a narrow range of $0.25 - 0.35$ when the radio is not very strong. However, in some observations, we require higher values of N, when the jet is also found to be stronger, i.e., observed radio flux density is high. When the jet is active, its contribution to X-rays also increases. Thus, the total X-ray flux (F_X) obtained from $3 - 25$ keV RXTE/PCA data is the sum total of the contribution both from the jets as well as from the accretion disk. On 2011 Oct. 22 (MJD $= 55856$), N was found to be 0.25 which is the lowest value. This leads us to assume that on this date, the X-ray flux is completely from the accretion disk (see JCD17). To estimate the X-ray contribution only from the accretion disk or inflowing matter ($F_{\rm inf}$), we refit all the spectra with N frozen at 0.25. By taking the differences between F_X (which is the flux in $3 - 25$ keV of our previous model fitted spectra, when all model parameters are kept free) and $F_{\rm inf}$ (which is the flux of our later fits with fixed $N = 0.25$) we can estimate the jet X-ray flux ($F_{\rm ouf}$) to be given by,

$$F_{\rm ouf} = F_X - F_{\rm inf}. \quad (1)$$

We have also calculated $F_{\rm ouf}$ during the 2012 outburst based on Swift/XRT analysis. From RXTE/PCA spectral analysis of the 2011 outburst, N was found to be minimum, $\sim 0.25 - 0.253$ from MJD $= 55850$ to 55867 during the declining phase of the hard state. This means that the X-ray jet must be lowest or inactive in these days (JCD17). The $0.5 - 10.0$ keV Swift/XRT spectrum of 2011 Oct. 25 (MJD $= 55859$) is now fitted with the TCAF model fits file to have an estimation of the model normalization at low or no X-ray jet condition for XRT spectrum in the specified energy band. For the best model fit, we find $N = 34.28$

(see Table 1). We also checked a few other XRT observations around 2011 Oct. 22 (MJD $= 55856$, with the minimum value of $N = 0.25$ in the $3 - 25$ keV PCA data), and found similar N values for the XRT. Thus, we used this Swift/XRT spectrum fitted N value (as there was no X-ray jet 'N' for XRT in $0.5 - 10.0$ keV for MAXI J1836–194) to calculate the jet X-ray flux for the 2012 outburst of the source. We freeze mass at $9.54\,M_{\odot}$ while fitting the XRT data. Note that F_X and $F_{\rm inf}$ fluxes for $3 - 25$ keV RXTE/PCA spectra are obtained using the 'flux 3.0 25.0' command, after retrieving the best model fits in XSPEC.

3 RESULTS

We study the source during its initial ~ 10 month (from 2011 August 31 to 2012 May 13; i.e., MJD $= 55804$ to 56060) period after its discovery on 2011 August 30. MAXI J1836–194 exhibited two outbursts in 2011 and 2012 with duration of ~ 3 and 2 months respectively, separated by ~ 4 months of quiescent period, during the period of our analysis. We compare variations of X-ray and radio intensities of the source, along with its spectral and jet properties.

3.1 X-ray and Radio Lightcurves

We plot $15 - 50$ keV Swift/BAT and $2 - 10$ keV MAXI/GSC fluxes in Figure 1(a)-(b). Hardness ratio (HR) of Swift/BAT and MAXI/GSC fluxes is displayed in Figure 1(c). HR is defined as the ratio between $15 - 50$ keV BAT and $2 - 10$ keV GSC rates. In Figure 1(d), radio flux densities in 5 and 7.45 GHz from the Very Large Array (VLA), and 5.5 GHz of ATCA data are displayed. Radio data are referenced from Russell et al. (2014b, 2015) papers.

The X-ray lightcurves (in Fig. 1(a)-(b)) are plotted for ~ 10 months between 2011 Aug 26 and 2012 Jun 7. In the rising phase of the 2011 outburst, both MAXI/GSC and Swift/BAT fluxes increased rapidly starting from 2011 Aug 29 (MJD $= 55802$). They attained a maximum peak flux around 2011 Sept 6 (MJD $= 55810$). After that, the flux decreased slowly, although Swift/BAT showed another small peak around 2011 Sept 9 (MJD $= 55813$). Both the 2011 and 2012 outbursts could be termed as 'Fast-Rise-Slow-Decay' (FRSD) type of variation in the outburst profiles (Debnath et al. 2010). From the spectral evolution, it could be denoted as 'type-II' or 'harder type' of BH binaries, since it does not show softer spectral states during its outbursts (Debnath et al. 2017). The BHC MAXI J1836–194 was active for ~ 3 months till MJD ~ 55890 during its 2011 outburst. Then it entered the quiescent state, which continued for ~ 4 months. The X-ray flux again started to rise around 2012 March 12 (MJD $= 55998$; Krimm et al. 2012; Yang et al. 2012a). The $15 - 50$ keV Swift/BAT flux increased significantly during this epoch of the 2012 outburst, although $2 - 10$ keV MAXI/GSC flux did not show any significant change. The 2012 outburst is much weaker compared to the 2011 outburst and it continued for ~ 2 months. On 2012 March 24 (MJD $= 56010$), maximum flux in Swift/BAT was observed. During this outburst, BAT flux rapidly increased for the initial ~ 20 d before it decreased. After that, it moved to the quiescent phase, where the flux remained almost constant at very low values.

HR roughly indicates whether a BHC is in the SS or in the hard state. During the 2011 outburst, HR was minimum on MJD ~ 55820. The BHC was in the hard-intermediate state (HIMS) during that time (see Paper-I). Paper-I also demonstrated that the accretion rate ratio intensity diagram (ARRID) is a better alternative to the 'q'-diagram or hardness intensity diagram (HID) as in Ferrigno et al. (2012) for describing transitions between spectral states. For a quick look, HR is more useful since to obtain ARRID, one needs to fit spectra with the TCAF model. From Figure 1(c), we observe that at the very beginning of the 2011 outburst, HR increased rapidly, before it started to decrease slowly until MJD $= 55820$. After that, HR increased slowly and varied within $\sim 1 - 6$. This trend of higher (hard state) HR value continued more or less in the quiescent state as well as in the 2012 outburst. In the quiescent state, HR fluctuated between 2 and 6, which implies that during the quiescent state, the source was in the hard state with a very low mass accretion rate. During the 2012 outburst, the same HR was observed. However, to check if during the entire 2012 outburst period the object remained in a hard state, we need to carry out the spectral analysis.

3.2 Accretion Flow Properties of MAXI J1836–194

We study accretion flow properties of MAXI J1836–194 during its 2011 and 2012 outbursts, and the intervening quiescent phase. The detailed spectral and timing analysis relying on RXTE/PCA data to infer accretion flow dynamics of the source during its 2011 outburst has already been reported in Paper-I. Here, we extend our analysis period to cover quiescence as well as the 2012 outburst, wherever the data are available. We mainly concentrate on the properties of the jet in X-rays.

3.2.1 2011 outburst

As stated earlier, the detailed study of the spectral and timing analysis to infer the accretion flow dynamics of the source during this outburst has already been reported in Paper-I using $2.5 - 25$ keV RXTE/PCA data. Based on the variation of accretion rate ratio (ARR $= \dot{m}_h/\dot{m}_d$), nature

Table 1 Swift/XRT Results Fitted with the TCAF Solution

Obs ID	MJD (Day)	$\dot{m}_d$ ($\dot{M}_{\rm Edd}$)	$\dot{m}_h$ ($\dot{M}_{\rm Edd}$)	X_s (r_s)	R	N	Line E (keV)	χ^2/dof
(1)	(2)	(3)	(4)	(5)	(6)	(7)	(8)	(9)
00032087028	55859.21	$1.698^{\pm 0.023}$	$0.584^{\pm 0.013}$	$73.19^{\pm 2.44}$	$1.081^{\pm 0.087}$	$34.21^{\pm 1.93}$	$6.33^{\pm 0.22}$	833.2/940
00032308002	56006.85	$0.011^{\pm 0.001}$	$0.162^{\pm 0.002}$	$281.22^{\pm 5.65}$	$3.567^{\pm 0.145}$	$74.92^{\pm 2.23}$	$6.68^{\pm 0.19}$	760.3/940
00032308005	56013.05	$0.012^{\pm 0.001}$	$0.158^{\pm 0.002}$	$271.24^{\pm 6.22}$	$3.557^{\pm 0.129}$	$93.82^{\pm 1.91}$	$6.61^{\pm 0.14}$	755.7/940

First observation is from the 2011 outburst. Last two observations are from the 2012 outburst. Data analysis is done using $0.5-10.0$ keV Swift/XRT data with TCAF solution. Accretion rates ($\dot{m}_d$ and $\dot{m}_h$) are expressed in terms of Eddington accretion rate ($\dot{M}_{\rm Edd}$). Shock location (X_s) is presented in Schwarzschild radius (r_s). R is the compression ratio (ratio of post-shock density to pre-shock density). Mass is kept frozen at $9.54\,M_\odot$. N is TCAF normalization. Gaussian 'line E' represents peak energy of Fe$-k_\alpha$ line.

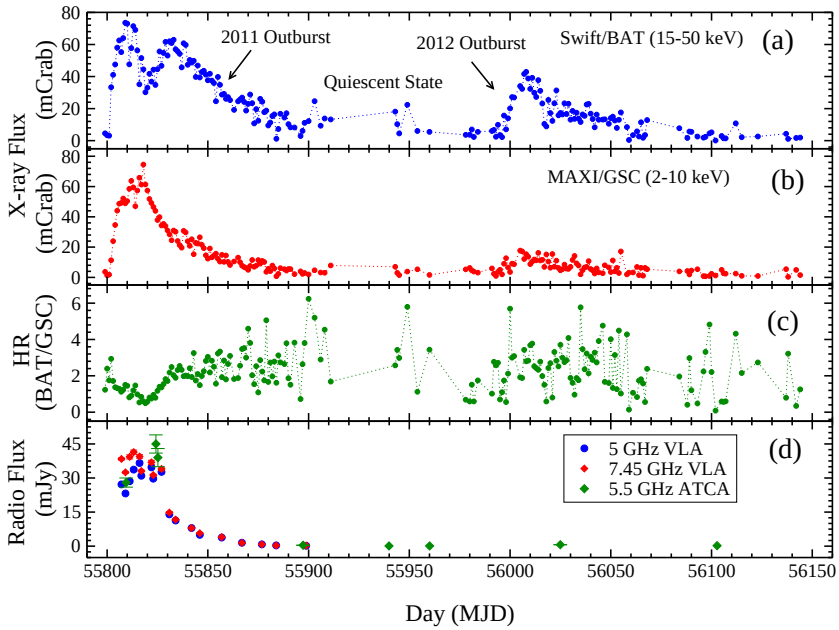

Fig. 1 Variation of (a) $15-50$ keV Swift/BAT flux in mCrab, (b) $2-10$ keV MAXI/GSC flux in mCrab, (c) HR $=15-50$ keV BAT/($2-10$ keV) GSC rates), and (d) 5 GHz VLA, 5.5 GHz ATCA and 5.5 GHz VLA radio flux densities in the unit of mJy are shown. Radio data are taken from Russell et al. (2015). The 2011 outburst began on MJD $=55804$ and continued for ~ 3 months till MJD ~ 55890. The 2012 outburst began on MJD $=56000$ and remained active for ~ 2 months. In between the 2011 and 2012 outburst, the source was in the quiescent state for ~ 4 months.

of QPOs, they classified the entire outburst into two spectral states: hard state (HS) and HIMS. These observed states form a hysteresis loop as: HS (Ris.) $\rightarrow$ HIMS (Ris.) $\rightarrow$ HIMS (Dec.) $\rightarrow$ HS (Dec.). No signature of the softer spectral states, i.e., soft-intermediate state (SIMS) and SS was observed. Since the source is one of the shorter orbital period BHCs, there could be a high amount of low angular momentum halo component from the companion winds, hardening the flow. From the spectral analysis, Jana et al. (2016) estimated the probable mass of BH to be in the range of $7.5-11.0\,M_\odot$. Taking the average, the probable mass of the BH is about $9.54^{+1.47}_{-2.03}\,M_\odot$. They also estimated the viscous time scale as ~ 10 d, obtained from the differences in occurrences of the peaks of two types of accretion rates ($\dot{m}_d$ and $\dot{m}_h$).

While fitting the spectra with the TCAF model fits file, Jana et al. (2016) did not find the model normalization (N) to be roughly constant throughout the outburst. Generally it varied within $0.25-0.35$. However, in some observations, very high N values were required to fit the spectra, particularly when the radio flux densities were high. This indicates that these higher values of N may be due to the excess contribution of the X-rays from the jets (JCD17). We apply the same method as in JCD17 to obtain the X-ray flux of the jet in the present object.

3.2.2 Quiescent state

In general, a BHC is considered to be in quiescent state when the X-ray luminosity $L_X<10^{34}$ erg s^{-1} (Remillard & McClintock 2006). It is believed that the quiescent state is the extended phase of hard/low-hard state with very low accretion rate and low luminosity. MAXI J1836–194 was in the quiescent state for ~ 4 months between its 2011 and

2012 outbursts. X-ray luminosity in the $2-10$ keV band (calculated from MAXI/GSC observed flux) was observed as low as $L_X \sim 10^{33}$ erg s^{-1} during the phase. HR was observed to be higher (in between $\sim 2-6$). The radio jet was observed during this phase though the luminosity was much lower as compared to the 2011 outburst. The nature of the X-ray flux, observation of radio flux and higher HR indicate that MAXI J1836–194 was in the hard/low-hard state during this phase with very low accretion rate.

3.2.3 2012 outburst

The 2012 outburst was much weaker as compared to the 2011 outburst. Luminosity was about one hundred times lower than that of the 2011 outburst. This new flaring activity of MAXI J1836–194 was detected by Swift/BAT on 2012 March 10 (Krimm et al. 2012). The source was active for about ~ 60 d. Grebenev et al. (2013) reported that the $0.3-400$ keV Swift+INTEGRAL spectra are PL dominated with very little contributions from the DBB component. We have analyzed Swift/XRT spectra in the energy range of $0.5-10.0$ keV with the TCAF model, though due to the lack of data points and low signal-to-noise ratio, we are unable to achieve acceptable χ^2-statistics in many observations with TCAF model or with the phenomenological DBB plus PL models. We only found better χ^2 statistics in two observations on 2012 March 20 (MJD $= 56006$) and 2012 March 27 (MJD $= 56013$). Model fitted parameters of these two XRT observations are listed in Table 1.

The TCAF model fitted extracted values and high values of ARR suggest that the disk is highly dominated by the sub-Keplerian halo component. The sub-Keplerian halo rate ($\dot{m}_h$) is found to be much higher as compared to the Keplerian disk rate ($\dot{m}_d$), so ARRs are also observed to be high ($\sim 13-14$). The 2012 outburst was dominated by the low viscous sub-Keplerian matter similar to the 2011 outburst of MAXI J1836–194. So, we can assume that the viscosity parameter was lower than the critical value during the entire period of the outburst. If viscosity was above the critical value, the sub-Keplerian flow would have been converted to a Keplerian disk (Chakrabarti 1990a,b, 1996 and references therein). Due to this, a low supply in Keplerian disk component is observed, which was unable to cool the CENBOL sufficiently. Thus, the source did not enter in the softer spectral state. Higher values of the TCAF model normalization (74.92 and 93.82) indicate that the X-ray contribution of the jet could be strong as well. But unfortunately, there was no radio observation in the period between MJD $= 55961-56023$. Note, during the spectral fitting, we kept mass of the BH frozen at $9.54\,M_\odot$.

3.3 Disk-Jet Connections

3.3.1 Evolution of jets

In the TCAF paradigm which is originated from viscous transonic flow solutions, jets are produced from the CENBOL. This implies that both Comptonized radiation from the CENBOL region and the base of the jet would contribute to the accretion disk spectra and the jet spectra respectively, with the latter being important only when the jets are active. This feature of the TCAF was exploited in JCD17 for Swift J1753.5–0127 while separating the X-ray spectrum of the jet from the total X-ray spectrum observed by satellites. Later, this method was employed to estimate the jet X-ray flux for another transient BHC XTE J1118+480 during its 2000 outburst (Chatterjee et al. 2019a). This motivated us to re-look into MAXI J1836–194 (Paper-I) where the deviation of the constancy of the model normalization was observed, i.e., when higher N values are required to fit the spectra in highly luminous HIMS. In these high N valued observations, observed radio fluxes were also reported to be higher (Russell et al. 2014b, 2015). Using the procedure of JCD17, the X-ray contributions from the jet during the 2011 and 2012 outbursts are obtained (see Table 2). The variation of total X-ray flux (F_X), accretion disk X-ray flux ($F_{\rm inf}$) and jet X-ray flux ($F_{\rm ouf}$) are displayed in Figure 2(a)-(c). The variation of the TCAF fitted normalization (N) is shown in Figure 2(d). Also, 7.45 GHz VLA radio data are plotted in Figure 2(e). The jet X-ray flux ($F_{\rm ouf}$) is found to increase slowly as the day progresses during the 2011 outburst, and it attained the maximum value on $\sim$ 2011 Sept. 9 (MJD $= 55813$). VLA first observed the source in 7.45 GHz radio band on 2011 Sept. 3 (MJD $= 55807$), with a flux density of 27 mJy. It was roughly constant for the next ~ 20 d. The source was in the HIMS during this phase of the outburst. $F_{\rm ouf}$ also exhibited roughly constant nature in this state. $F_{\rm ouf}$ started to decrease after 2011 Sept. 23 (MJD $= 55827$). Radio flux density also manifested a similar behavior. The BHC entered into the HS (Dec.) on 2011 Oct. 1 (MJD $= 55835$), which continued till the end of the outburst. During this phase of the outburst, both $F_{\rm ouf}$ and F_R were found to be very low.

TCAF normalization (N) also showed a similar behavior as F_R and $F_{\rm ouf}$. It increased slowly in the rising phase of the 2011 outburst. On MJD $= 55813.56$ and 55818.84, much higher N values of 1.99 and 2.07 respectively were required to fit the spectra with the TCAF fits file. After that, N decreased slowly till MJD $\sim$ 55830 after which N varied within a narrow range of $\sim 0.25-0.35$. Four spectra from different spectral states are depicted in Figure 3(a)-(d). The spectra are fitted with free (black solid curves) or frozen (at 0.25; red dashed curves) normalization values.

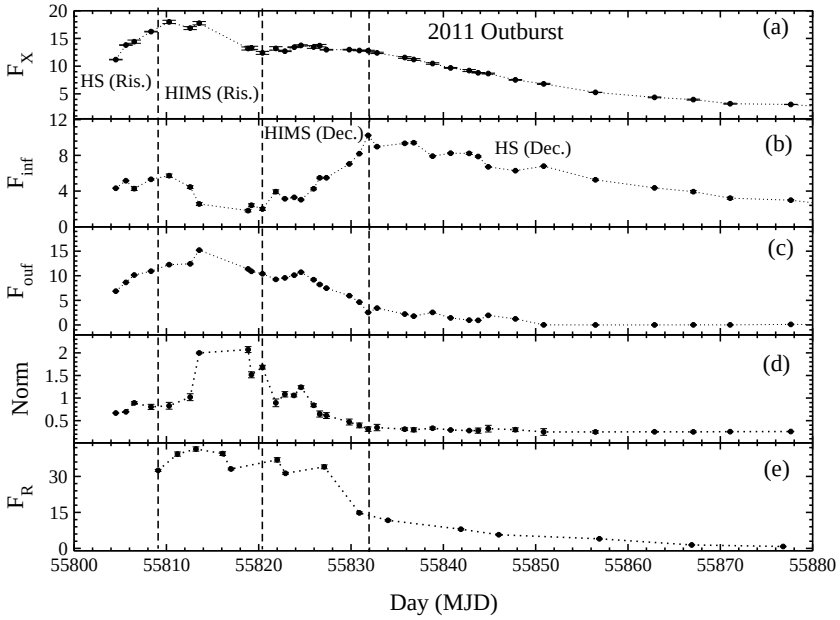

Fig. 2 Variations of (a) total X-ray flux (F_X), (b) the X-ray flux from accretion disk ($F_{\rm inf}$), (c) the jet X-ray flux ($F_{\rm ouf}$), (d) TCAF normalization (N) and (e) 7.45 GHz radio flux density (F_R) of VLA observation are displayed with day (MJD) during the 2011 outburst. The radio data are referenced from Russell et al. (2014b, 2015). X-ray flux is in the RXTE/PCA energy range of $3-25$ keV and in the unit of 10^{-9} erg cm^{-2} s^{-1}.

The jet spectra are obtained by taking differences between them and signified with a blue dash-dotted curve. We can see that the jet spectra are stronger in the HIMS and also they are harder than the disk spectra.

We have also analyzed a few Swift/XRT spectra from the 2011 outburst in between MJD $=$ 55850 and 55867, when TCAF normalization values are $(0.25-0.253)$ around the minimum normalization ($N=0.25$ on MJD $=55856$) in $3-25$ keV RXTE/PCA. For $0.5-10$ keV XRT data, the fitted model normalizations are found to be $\sim N=35$. No XRT observations were available on the day when the PCA N was minimum. In Table 1, we provide the Swift/XRT model fitted result on 2011 Oct. 25 (MJD $=55859$), when the minimum $N=34.28$ for XRT in $0.5-10$ keV was required. During the 2012 outburst, due to low signal-to-noise ratio of the XRT data, we find better χ^2 statistics only in two observations, on MJD $=56006$ and 56013, when $0.5-10.0$ keV XRT fluxes were observed at 2.20×10^{-10} and 2.35×10^{-10} erg cm^{-2} s^{-1} respectively. To estimate the X-ray contributions only from the accretion disk, we refitted both the spectra by keeping N frozen at 34.28. Taking differences of the previous (when all model parameters are kept free) and present model fitted fluxes, we calculate the jet/outflow contribution in the X-rays. Jet X-ray fluxes are found to be 1.195×10^{-10} and 1.493×10^{-10} erg cm^{-2} s^{-1} on MJD $=$ 56006 and 56013 respectively.

MAXI J1836–194 exhibited strong jet activity during its 2011 outburst as compared to Swift J1753.5–0127 during its 2005 outburst. When the jet was the strongest in the HIMS of the 2011 outburst, its contribution in X-ray is found to be up to $\sim$86%. On average, the jet X-ray contributed $\sim$41% throughout the 2011 outburst. In the 2012 outburst, its contribution is found to be $\sim$54% and $\sim$63% in the two observations we studied, although total X-ray fluxes are much lower than those of the 2011 outburst (see Table 2).

3.3.2 Radio and X-ray flux correlations

Standard jet models predict a correlation between the radio and X-ray luminosity (Falcke & Biermann 1995; Heinz & Sunyaev 2003; Markoff et al. 2003; Russell et al. 2013). It was first observed for BHC GX 339-4 (Hannikainen et al. 1998). Several BHCs show a standard correlation $F_R\sim F_X^b$ in the HS, with a correlation index of $b\sim0.5-0.7$ (Corbel et al. 2003, 2013; Gallo et al. 2003, 2004, 2006). The correlation has been extended to the quiescent state (Gallo et al. 2014; Plotkin et al. 2013, 2017). The correlation is extended to AGNs in the so-called 'fundamental plane of black hole activity' by including the mass and accretion rate (Merloni et al. 2003; Heinz 2004; Kording et al. 2006). However, some BHCs manifest a steeper index ~1.4 (Coriat et al. 2011; Jonker et al. 2012). A few other BHCs exhibit dual correlation tracks. H 1743–322, XTE J1752–223 and MAXI J1659–152 are some sources, where steeper correlation indices are observed when L_X $>10^{36}$ erg s^{-1}. However, they are found to move towards

Table 2 X-ray Jet during 2011 and 2012 Outburst

No. (1)	Obs ID (2)	MJD (3)	N (4)	F_X (5)	$F_{\rm inf}$ (6)	$F_{\rm ouf}$ (7)	% of $F_{\rm ouf}$ (8)
1	X-01-00	55804.52	$0.669^{\pm 0.002}$	$11.181^{\pm 0.052}$	$4.318^{\pm 0.041}$	$6.863^{\pm 0.011}$	61.38
2	X-02-00	55805.61	$0.695^{\pm 0.002}$	$13.811^{\pm 0.049}$	$5.159^{\pm 0.035}$	$8.652^{\pm 0.014}$	62.64
3	X-03-00	55806.51	$0.893^{\pm 0.027}$	$14.417^{\pm 0.290}$	$4.276^{\pm 0.212}$	$10.141^{\pm 0.078}$	70.34
4	X-03-01	55808.33	$0.804^{\pm 0.057}$	$16.235^{\pm 0.057}$	$5.313^{\pm 0.071}$	$10.922^{\pm 0.014}$	67.27
5	X-03-02	55810.29	$0.829^{\pm 0.076}$	$17.985^{\pm 0.301}$	$5.725^{\pm 0.192}$	$12.260^{\pm 0.104}$	68.16
6	X-03-03	55812.57	$1.020^{\pm 0.077}$	$16.865^{\pm 0.271}$	$4.451^{\pm 0.156}$	$12.414^{\pm 0.096}$	73.60
7	Y-01-00	55813.55	$1.998^{\pm 0.017}$	$17.755^{\pm 0.299}$	$2.554^{\pm 0.162}$	$15.201^{\pm 0.077}$	85.61
8	Y-01-04	55818.84	$2.073^{\pm 0.066}$	$13.185^{\pm 0.281}$	$1.807^{\pm 0.147}$	$11.378^{\pm 0.134}$	86.29
9	Y-01-05	55819.20	$1.515^{\pm 0.067}$	$13.308^{\pm 0.283}$	$2.413^{\pm 0.167}$	$10.895^{\pm 0.116}$	81.86
10	Y-02-03	55820.40	$1.683^{\pm 0.042}$	$12.394^{\pm 0.271}$	$1.993^{\pm 0.152}$	$10.401^{\pm 0.119}$	83.92
11	Y-02-00	55821.85	$0.894^{\pm 0.085}$	$13.198^{\pm 0.315}$	$3.933^{\pm 0.209}$	$9.265^{\pm 0.106}$	70.19
12	Y-02-01	55822.83	$1.083^{\pm 0.059}$	$12.699^{\pm 0.078}$	$3.139^{\pm 0.051}$	$9.560^{\pm 0.027}$	75.28
13	Y-02-04	55823.84	$1.059^{\pm 0.031}$	$13.416^{\pm 0.075}$	$3.296^{\pm 0.042}$	$10.119^{\pm 0.029}$	75.43
14	Y-02-05	55824.58	$1.240^{\pm 0.033}$	$13.751^{\pm 0.102}$	$3.033^{\pm 0.054}$	$10.718^{\pm 0.056}$	77.94
15	Y-02-02	55825.94	$0.841^{\pm 0.033}$	$13.453^{\pm 0.242}$	$4.256^{\pm 0.102}$	$9.197^{\pm 0.130}$	68.36
16	Y-02-06	55826.60	$0.647^{\pm 0.068}$	$13.701^{\pm 0.223}$	$5.481^{\pm 0.088}$	$8.220^{\pm 0.112}$	59.99
17	Y-03-04	55827.33	$0.613^{\pm 0.065}$	$12.962^{\pm 0.071}$	$5.488^{\pm 0.050}$	$7.474^{\pm 0.021}$	57.66
18	Y-03-01	55829.80	$0.470^{\pm 0.066}$	$12.984^{\pm 0.061}$	$7.043^{\pm 0.028}$	$5.941^{\pm 0.033}$	45.75
19	Y-03-05	55830.89	$0.395^{\pm 0.053}$	$12.826^{\pm 0.057}$	$8.189^{\pm 0.024}$	$4.637^{\pm 0.037}$	36.15
20	Y-03-02	55831.84	$0.313^{\pm 0.050}$	$12.785^{\pm 0.091}$	$10.241^{\pm 0.035}$	$2.544^{\pm 0.056}$	19.89
21	Y-03-03	55832.81	$0.348^{\pm 0.070}$	$12.396^{\pm 0.122}$	$8.976^{\pm 0.064}$	$3.420^{\pm 0.058}$	27.58
22	Y-04-01	55835.81	$0.311^{\pm 0.031}$	$11.557^{\pm 0.152}$	$9.345^{\pm 0.078}$	$2.212^{\pm 0.084}$	19.13
23	Y-04-02	55836.78	$0.298^{\pm 0.044}$	$11.201^{\pm 0.154}$	$9.417^{\pm 0.098}$	$1.784^{\pm 0.096}$	15.92
24	Y-04-04	55838.83	$0.333^{\pm 0.025}$	$10.473^{\pm 0.140}$	$7.914^{\pm 0.071}$	$2.559^{\pm 0.069}$	24.43
25	Y-04-06	55840.78	$0.294^{\pm 0.007}$	$9.678^{\pm 0.079}$	$8.246^{\pm 0.058}$	$1.432^{\pm 0.021}$	14.79
26	Y-05-00	55842.79	$0.280^{\pm 0.008}$	$9.200^{\pm 0.179}$	$8.217^{\pm 0.118}$	$0.982^{\pm 0.067}$	10.67
27	Y-05-01	55843.76	$0.280^{\pm 0.057}$	$8.805^{\pm 0.045}$	$7.869^{\pm 0.071}$	$0.936^{\pm 0.026}$	10.62
28	Y-05-04	55844.86	$0.323^{\pm 0.074}$	$8.666^{\pm 0.084}$	$6.714^{\pm 0.037}$	$1.952^{\pm 0.057}$	22.52
29	Y-05-06	55847.80	$0.300^{\pm 0.042}$	$7.518^{\pm 0.069}$	$6.283^{\pm 0.025}$	$1.235^{\pm 0.044}$	16.42
30	Y-06-02	55850.87	$0.251^{\pm 0.074}$	$6.805^{\pm 0.097}$	$6.794^{\pm 0.041}$	$0.011^{\pm 0.056}$	0.16
31	Y-07-00	55856.47	$0.250^{\pm 0.027}$	$5.263^{\pm 0.014}$	$5.263^{\pm 0.087}$	$0.000^{\pm 0.073}$	0.00
32	Y-08-00	55862.87	$0.253^{\pm 0.011}$	$4.367^{\pm 0.075}$	$4.358^{\pm 0.024}$	$0.008^{\pm 0.099}$	0.19
33	Y-08-05	55867.08	$0.252^{\pm 0.016}$	$3.956^{\pm 0.087}$	$3.935^{\pm 0.132}$	$0.021^{\pm 0.055}$	0.54
34	Y-09-02	55871.06	$0.256^{\pm 0.007}$	$3.216^{\pm 0.088}$	$3.205^{\pm 0.125}$	$0.010^{\pm 0.037}$	0.31
35	Y-10-01	55877.63	$0.259^{\pm 0.002}$	$3.085^{\pm 0.022}$	$2.978^{\pm 0.077}$	$0.107^{\pm 0.055}$	3.47
36	00032308002*	56006.85	$74.92^{\pm 2.23}$	$2.201^{\pm 0.023}$	$1.101^{\pm 0.012}$	$1.193^{\pm 0.011}$	54.23
37	00032308005*	56013.05	$93.87^{\pm 1.99}$	$2.353^{\pm 0.024}$	$0.859^{\pm 0.010}$	$1.493^{\pm 0.014}$	63.48

F_X, $F_{\rm ouf}$ and $F_{\rm inf}$ are the unit of 10^{-10} erg cm^{-2} s^{-1}. For the 2011 outburst, F_X, $F_{\rm ouf}$ and $F_{\rm inf}$ are calculated in the energy range of $3-25$ keV. For the 2012 outburst, fluxes are calculated in $0.5-10.0$ keV energy range. $F_{\rm ouf}/F_X$ indicate % of jet X-ray contributions out of total X-rays. X =96371-03, Y =96438–01 are prefixes of observation ID's. * are from the 2012 outburst.

the standard correlation track in the low luminosity state (Jonker et al. 2010, 2012; Coriat et al. 2011; Ratti et al. 2012), but Swift J1753.5–0127 has shown a different correlation index ($b \sim 1$) (Soleri et al. 2010; Rushtan et al. 2016, JCD17).

Interestingly, these correlations of F_R have been obtained with total X-ray flux (F_X) in the $3-9$ keV band, which contains X-ray fluxes both from the disk and the jet. This may be the reason for different correlation indices in different spectral states of the same source. Since we have been able to separate the X-ray contributions of the jet ($F_{\rm ouf}$) and the accretion disk ($F_{\rm inf}$) from the total X-rays, correlation curves between F_R with $F_{\rm ouf}$ and $F_{\rm inf}$, could be plotted. In Figure 4(a), the plot between F_R and $F_{\rm ouf}$ (in $3-25$ keV) is shown, where the correlation index is found to be $b = 0.61 \pm 0.08$, which is within the limit of standard correlation. Here, we have used 7.45 GHz VLA flux as F_R. For Swift J1753.5–0127, a similar correlation index ($b = 0.59 \pm 0.11$) between F_R and $F_{\rm ouf}$ was also found (see, JCD17 for more details). This indicates that the mechanism for jet production could be the same, at least for these two BHCs.

We have also drawn a plot of F_R vs F_X for MAXI J1836–194 during its 2011 outburst in Figure 4(c)-(d) and it is fitted with $F_R \sim F_X^b$ to find the correlation index. For $3-25$ keV PCU2 flux (F_X), we find $b \sim 1.79 \pm 0.11$. Similarly, when we utilize $3-9$ keV PCU2 flux (F_X), $b \sim 1.82 \pm 0.12$. Russell et al. (2015) also reported a similar steeper correlation index ($b \sim 1.8 \pm 0.2$). Interestingly, we did not find any correlation between F_R and $F_{\rm inf}$ (see, Fig. 4(b)).

In Figure 5, we draw the correlation plot in luminosity, i.e., the $L_R - L_X$ plane. Other than the 2011 outburst of MAXI J1836–194, data from the 2012 outburst and the

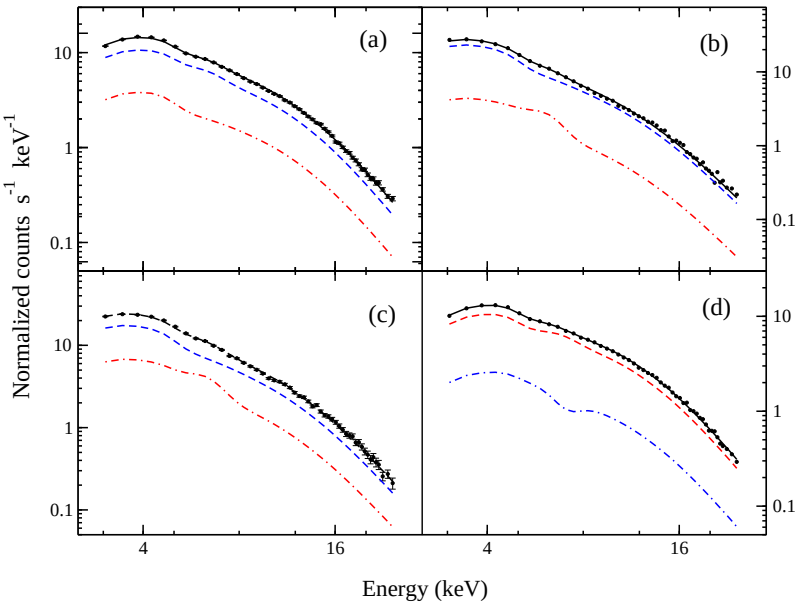

Fig. 3 Four spectra selected from four different spectral states, fitted with the TCAF model fits file by keeping model normalization free (*blue curves*) or frozen at $N = 0.25$ (*red curves*). The spectra are from observation IDs: (a) 96371–03–01–00 (HS - Ris.), (b) 96438–01–01–04 (HIMS - Ris.), (c) 96438–01–02–00 (HIMS - Dec.) and (d) 96438–01–04–01 (HS - Dec.). Jet X-ray spectra are depicted in *blue dash-dotted curves*.

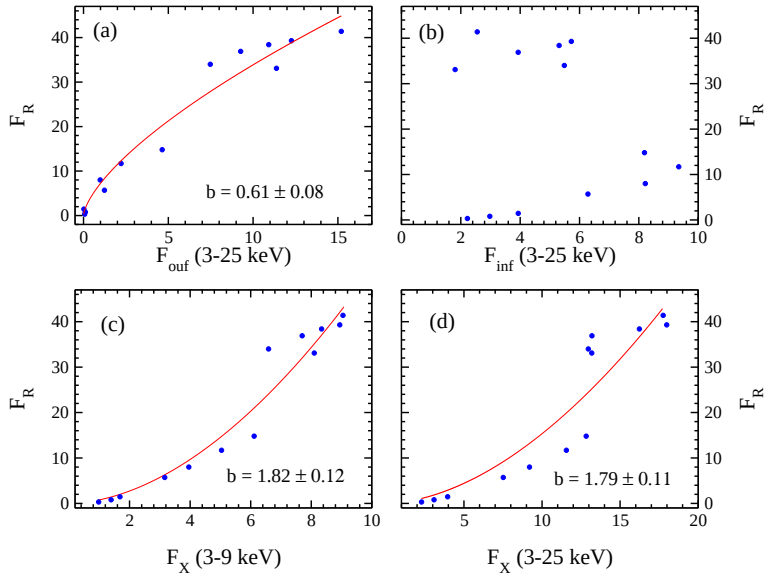

Fig. 4 Correlation plots are depicted for 7.45 GHz F_R with (a) $3-25$ keV $F_{\rm ouf}$, (b) $3-25$ keV $F_{\rm inf}$, (c) $3-9$ keV F_X and (d) $3-25$ keV F_X. The correlations are in the form of $F_R \sim F_X^b$, where b is the correlation index. We did not find any correlation between F_R and $F_{\rm inf}$. F_R is in the unit of mJy. F_X, $F_{\rm ouf}$ and $F_{\rm inf}$ are in the unit of 10^{-10} erg cm^{-2} s^{-1}.

quiescent state between two outbursts are also included. As stated earlier, during the 2012 outburst, acceptable χ^2-statistics are achieved only for two observations. We calculated the jet X-ray contribution on these two days but no quasi-simultaneous radio data are available for these two observations. So, we are unable to include these two results in the plot. We only display variation of the total X-rays (L_X in $2-10$ keV) with L_R. For the 2011 outburst of MAXI J1836–194 and the 2005 outburst of Swift J1753.5–0127, we utilize the TCAF model fitted spectral result of RXTE/PCA from Paper I and JCD17 respectively. For the quiescent state as well as for the 2012 outburst of MAXI J1836–194, we employ $2-10$ keV MAXI/GSC data for calculating L_X values, where radio data are available. It can be noted that two data points from the quiescent state and one data point from the 2012 outburst are not actual detections, but rather they are upper limits of the radio flux (Russell et al. 2014b, 2015). We also calculate the jet

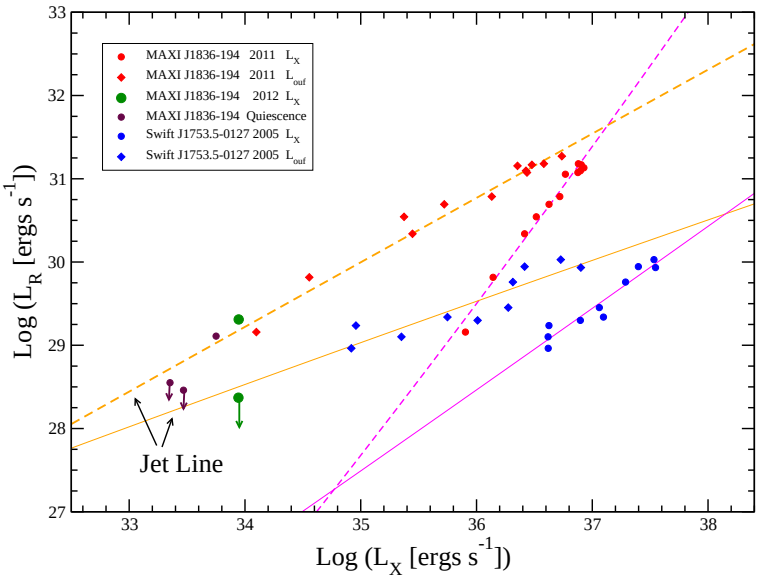

Fig. 5 Correlation plots are depicted in the luminosity plane. *Orange dashed* and *solid lines* delineate the correlation track of $L_R - L_{\rm ouf}$ for MAXI J1836–194 during the 2011 outburst and Swift J1753.5–0127 during the 2005 outburst respectively. *Red* and *blue diamonds* mark $L_R - L_{\rm ouf}$ points for MAXI J1836–194 and Swift J1753.5–0127 respectively. *Red* and *blue circles* mark $L_R - L_X$ correlation points for MAXI J1836–194 during the 2011 outburst and Swift J1753.5–0127 during the 2005 outburst respectively. *Purple dashed* and *solid lines* are for the $L_R - L_X$ correlation track for MAXI J1836–194 during the 2011 outburst and Swift J1753.5–0127 during the 2005 outburst respectively. *Green* and *brown circles* represent $L_R - L_X$ points for MAXI J1836–194 during the 2012 outburst and quiescent state respectively. Note: X-ray luminosities (L_X) are calculated in the $2 - 10$ keV range of PCA and XRT by assuming the distance of MAXI J1836–194 and Swift J1753.5–0127 to be 7 kpc and 8 kpc respectively. '*Down arrows*' indicate points with upper limit of the radio luminosities.

X-ray luminosity ($L_{\rm ouf}$) for MAXI J1836–194 (during its 2011 outburst) as well as for Swift J1753.5–0127 (during its 2005 outburst) using TCAF model fitted PCA spectra. We find that the quiescent and 2012 outburst data (L_X) points lie on the correlation track of jet ($L_R - L_{\rm ouf}$) instead of their total X-ray track ($L_R - L_X$). This indicates that there was very little contribution in the X-rays from the accretion disk or inflowing matter. Only the jet contributes in X-rays during the 2012 outburst as well as in the quiescent state. However, three upper limit points indicate that actual radio fluxes could be at a lower level and may fall close to the $L_R - L_X$ line.

In the case of compact jets, we expect a tight correlation between F_R and $F_{\rm ouf}$. For discrete ejections, a tight correlation may not be found. For BHC Swift J1753.5–0127, a tight correlation is not obtained, especially in the HIMS when flux was much higher. In the HIMS, the nature of the jet is not entirely compact and perhaps partially blobby (see JCD17 and references therein). For MAXI J1836–194, a tight correlation is obtained for F_R and $F_{\rm ouf}$ during both HS and HIMS. This indicates that the nature of the jet is compact for this BHC, though the possibility of fast and slow components cannot be ruled out. Russell et al. (2015) also reported the compact nature of the jet for this BHC.

4 DISCUSSIONS AND CONCLUDING REMARKS

Considering the fact that the TCAF model normalization is a constant for a given source and observing instrument, fits with good quality data are expected to have constant normalization. However, normalization may have small fluctuations due to an error in the model fittings or data quality, but any significant deviation indicates the presence of other physical processes such as jet, disk precession, etc. which are not included in TCAF based fits file used here. In this present paper, N varied between $\sim 0.25 - 0.35$ in the low activity radio phase with minimum value of $N = 0.25$. But in the higher jet activity period (in HIMS), observed N values ($\sim 1.5 - 2.1$) are found to be $\sim 6 - 8$ times greater than minimum N. So, the continuous (not in a random single observation) of higher N values is certainly not due to instrumental/modelling error. Rather, they appear to be due to the jet activity.

Since the base of the jet/outflow also contributes to X-ray along with the accretion disk, in a jet dominated phase, a higher value of normalization is expected. This allows us to segregate the contributions from the inflow and outflow components. During the 2011 outburst of MAXI J1836–194, N is generally varied between $0.25 - 0.35$, except for the days with jet domination, when much higher N values are required to fit the spectra satisfactorily. As in JCD17, here we also assume that only accretion disk or inflowing

matter contributes in the X-rays when the minimum value of $N = 0.25$ was required (as on 2011 Oct. 22, MJD $= 55856$) while fitting $3 - 25$ keV RXTE/PCA data of MAXI J1836 during its 2011 outburst. Though the radio jet appeared to be weakly active on this day, we assumed that contribution of the jets to the X-ray was negligible. To estimate the X-ray flux contributions coming only for the accretion disk or inflowing matter ($F_{\rm inf}$), we refit all the spectra with N frozen at 0.25. Applying Equation (1), we calculate the jet contributions in X-rays ($F_{\rm ouf}$).

In the TCAF paradigm, spectral states are related to variation of the flow parameters including shock compression ratio (see Debnath et al. 2015a, 2017 and references therein). At the beginning of an outburst, generally a BH starts in the HS. In this HS, presence of a strong shock (with high R) located far away from the BH is seen. As the outburst progresses, the source enters into the intermediate state (HIMS and SIMS). In this state, due to rise in cooling rate (as number of soft photons increases with rise in $\dot{m}_d$), size of the CENBOL is reduced. So in these states, the shock becomes weaker and moves inward. The strength of the shock becomes intermediate. As the outburst progresses further, the source enters the SS. In this state, the shock becomes very weak or absent with $R \sim 1$. In the declining phase, opposite behaviors of the flow parameters are seen. Chakrabarti (1999a,b) predicted that the ratio of the outflow rate to inflow rate ($R_{\dot{m}}$) is maximum when the shock strength is intermediate. Chakrabarti (1999b) discussed the relation between spectral states and the outflow/inflow ratio (see fig. 2 of the Chakrabarti paper). Subsequently, it was made clearer in Chakrabarti (1999b, 2001, 2002) exactly when the jets would be most prominent. In the present case, we observed maximum jet X-ray flux ($F_{\rm ouf}$) in the HIMS for MAXI J1836–194, which is similar to the 2005 outburst of Swift J1753.5–0127 (see JCD17).

Jet kinetic power is converted to radiations in different wavebands (radio, infrared (IR), optical to X-ray). Russell et al. (2014b) showed that there is a significant contribution in the jet from IR and optical wavebands which is presumably due to synchrotron emission. However, since there is no real boundary between the CENBOL and the base of the jet, in $F_{\rm ouf}$, the dominating contribution could be due to inverse Comptonization and not due to the synchrotron process. Russell et al. (2014b) estimated jet luminosity ($L_{\rm jet}$) by integrating the jet spectra over $5 \times 10^9 - 7 \times 10^{14}$ Hz for six observations during the 2011 outburst. They ascertained $L_{\rm jet}$ was minimum in the HIMS though X-ray flux ($F_{\rm ouf}$) was higher. This indicates that the jet was active in the X-ray but not in the IR and optical. In the decay phase, the X-ray jet ($F_{\rm ouf}$) was found to decrease. This is expected since the accretion rate also decreased, which in turn reduced the mass outflow rate and jet X-ray flux ($F_{\rm ouf}$). This agrees with the theoretical point of view (C99a,b; Das & Chakrabarti 1999). However, Russell et al. (2014b) found $L_{\rm jet}$ increased in the decay phase. Radio flux was lower in this phase. Thus most of the jet power was emitted in the IR and optical wavebands with very little contribution in radio and X-ray (see Fig. 2 of this paper and fig. 2 of Russell et al. 2014b). In the decay phase, magnetic field at the base of the jet increased (Russell et al. 2014b). Due to high magnetic field, a significant amount of jet power was emitted in the IR and optical wavebands via synchrotron process. Since the jet is compact and dense, radio flux was very low due to high magnetic field. Thus, $L_{\rm jet}$ increased due to high IR and optical radiation while radio and jet X-ray fluxes were lower.

After $\sim$ 3 months of activity during the 2011 outburst, MAXI J1836–194 entered the quiescent state, which continued for the next $\sim$ 4 months. We calculated HR from $2 - 10$ keV MAXI/GSC and $15 - 50$ keV Swift/BAT lightcurves. HR is found to vary between $2 - 6$, indicating the source was in the harder states. Three ATCA observations were available at 5.5 GHz during the quiescent phase. However, radio flux densities were very low (~ 0.1 mJy). On the contrary, during the 2011 outburst, in the HIMS, 5.5 GHz ATCA flux density was ~ 40 mJy. X-ray luminosity (L_X) was also very low ($\sim 10^{33}$) during this phase. A radio jet is generally observed in the hard and intermediate spectral states. Observation of the radio jets and HR indicate that the source was in the low luminous HS during this phase of the outburst. However, there are some reports that the quiescent state spectra are softer than those of the HS for several other BHCs, such as XTE J1118+480 ($\Gamma \sim 2.02$), XTE J1550–564 ($\Gamma \sim 2.25$), GX 339–4 ($\Gamma \sim 1.99$) and V 404 Cyg ($\Gamma \sim 2.08$) (Corbel et al. 2006; Plotkin et al. 2013, 2017).

MAXI J1836–194 also manifested new flaring activity on 2012 March 12 (MJD $= 55998$), which continued for $\sim$ 2 months. We analyzed $0.5 - 10.0$ keV Swift/XRT spectra with the TCAF model and extracted accretion flow parameters for the two observations from MJD $= 56006.85$ and 56013.05. Our model parameters indicate the high dominance of the sub-Keplerian halo accretion rates and high shock strengths during these observations (see Table 1). This allowed us to infer that during the days we observed the 2012 outburst, the source was also in the HS. We also calculated jet contribution in the X-rays and found that the contributions were up to $\sim$54% and $\sim$63% of total X-ray in these two observations.

We expect $F_{\rm ouf}$ and F_R to be well correlated since they both originated from the jet. At the base of the jet, X-ray is emitted since it is the hottest region right above the CENBOL. As the jet moves away, it is cooled due to expansion. Hence, it emits in the other low energy waveband-

s, such as ultraviolet, IR and radio. The correlation between the disk and the jet X-rays should directly lead to correlations with other radiations from the jet. We have drawn a correlation plot between the jet X-ray flux in $3-25$ keV of RXTE/PCA and radio in 7.45 GHz VLA in Figure 4(a). We obtained the correlation in the form of $F_R \sim F_{\rm ouf}^{0.61\pm0.08}$. For Swift J1753.5–0127, a similar correlation of $F_R \sim F_{\rm ouf}^{0.59\pm0.11}$ is found. Thus, $F_R \sim F_{\rm ouf}^{0.6}$ could be a universal correlation, but to firmly establish it, we need more observations. Interestingly, Corbel et al. (2003, 2013) and Gallo et al. (2003) have found the standard correlation index to be $\sim 0.6-0.7$ if the correlation between F_R and F_X is examined. However, a steeper index ($\sim 1-1.4$) has been identified for many 'radio-quiet' BHCs (Jonker et al. 2012; Ratti et al. 2012). An unusually steep index is found for MAXI J1836–194 during its 2011 outburst when F_R was correlated with F_X. When we apply 7.45 GHz VLA data as F_R with $3-25$ keV RXTE/PCA flux as F_X, a steeper correlation is observed with index $b \sim 1.79 \pm 0.11$. Similarly, when we utilize $3-9$ keV RXTE/PCA flux as F_X, the index is found at $\sim 1.82 \pm 0.12$. A similar correlation was also reported by Russell et al. (2015). They suggested that it could be due to variable Lorentz factor throughout the outburst. Another possible reason behind these steeper correlation indices may be due to the high supply rate of low viscous sub-Keplerian matter in the form of wind or accretion, since it is a low orbital period (≤ 4.9 h) binary system. The system is very compact and its L1 point is closer to the BH as its mass is ~ 15 times higher than the companion. The rotational velocity of the accreting matter is high at L1, thus Coriolis force will be high on the inflowing stream of matter. This leads to a higher amount of deflection to part of the inflowing matter. This deflected stream of matter that is not accreted by the BH would form a hot cloud surrounding the accretion disk. Scatterings of photons emitted from the jets with this cloud of wind matter could steepen the correlation indices.

We have not found any correlation between $F_{\rm inf}$ and F_R (see Fig. 3(b)). It seems that this could be due to obscuration of the photons emitted from the pre-shock disk as well as from CENBOL. The obscuration suppresses the photon flux from the accretion disk or inflowing matter ($F_{\rm inf}$). In Figure 3(b), we clearly see that there are two branches. If we shift the upper branch toward the right (i.e., towards high flux), a correlation could be seen. However, due to the shift of the upper branch towards the lower side, we did not find any correlation. On the contrary, being a face-on system ($i = 4^\circ - 15^\circ$; Russell et al. 2014a), the jet may not be obscured. A strong correlation of $F_{\rm ouf}$ with F_R also confirms that there is low or negligible obscuration in the jet fluxes.

In the quiescent state, and the subsequent 2012 outburst, the $L_X - L_R$ correlation points lie in the $L_{\rm ouf} - L_R$ correlation track, i.e., jet-line of MAXI J1836–194 at lower L_X values. If the jet production mechanism remains the same across different outbursts, we may conclude that there was very little X-ray emission from the accretion disk in the quiescence and the 2012 outburst. All or most of the X-rays come from the jet or outflow. If this is true, then $L_X \sim L_{\rm ouf}$. Thus, it is possible that some alternate mechanism may exist for producing jets and outflows in the quiescent and low luminosity phases of these types of BH binary systems.

During the 2011 outburst, the jet contribution is as high as $\sim$86% of the total X-ray with an average contribution of $\sim$41%. This makes MAXI J1836–194 a jet dominated BHC. Even after the 2012 outburst, ATCA observed radio flux densities of 0.07 mJy at 5.5 GHz and 0.09 mJy at 9 GHz on MJD $= 56163$. This also indicates the activity of the jet on that day. Thus even when the X-ray luminosity is less than $\sim 10^{32}$ erg s^{-1}, the jet is active. Chakrabarti & Bhaskaran (1992) showed that it is easier to produce a jet from the sub-Keplerian halo. In the quiescent state, a Keplerian disk may not be formed due to the lack of viscosity. However, a constant supply of winds from the companion star form a radiatively inefficient sub-Keplerian flow which launches the jets. This implies that in the quiescent state as well as during the 2012 outburst, the X-ray contribution from the accretion disk is negligible.

High jet activity ($> 75\%$) of jet X-ray is quite unusual for transient stellar mass BH binaries, although, there are some observational evidences, such as SS 433 and XTE J1118+480, where high jet contributions were observed. In SS 433, it is believed that $\sim$100% of the X-ray flux was contributed by the jet since the accretion disk was obscured (Fabrika 2004 and references therein). In case of a short orbital period transient BHC XTE J1118+480, two outbursts (2000 and 2005) were induced by jet activity where the jet contributed as high as 75% in X-rays (Chatterjee et al. 2019a,b). Theoretically, a few models also support high jet activity such as advection dominated inflow-outflow solution (ADIOS; Blandford & Begelman 1999), jet dominated accretion flow (JDAF; Falcke & Markoff 2000; Markoff et al. 2001, 2003 and references therein) or the magnetically arrested disk (MAD; Narayan et al. 2003) model. In the ADIOS model, the outflow could be dominating if the accretion is radiatively inefficient and the accretion rate is low. The JDAF model infers that the broadband spectra, from radio to X-ray, are generated by synchrotron radiation from the jet. In the MAD model, energy extraction from the accreting matter is as high as 50% for a non-rotating BH in the presence of a strong magnetic field. But in the present case, we believe that obscuration of the accretion disk is

responsible for observing such high contribution from jet. In this case, the $F_{\rm inf}$ contribution would actually be larger than $\sim 14\%$ if there were no obscuring clouds and the relative jet contribution might be much less than the presently observed value of 86%.

$L_R - L_{\rm ouf}$ correlation is expected to hold tight as long as the jet remains compact. In case of a blobby jet or discrete ejection, we do not expect a tight correlation. For BHC Swift J1753.5–0127, we observe scatter points in the $L_R - L_{\rm ouf}$ track (see Fig. 5) especially in the HIMS. Thus, the nature of the jet for Swift J1753.5–0127 is blobby in the HIMS. However in HS, when the fluxes are low, a tighter correlation is obtained. It indicates that the jet remains compact as in the HS of Swift J1753.5–0127 during its 2005 outburst (JCD17). From Figure 5, for MAXI J1836–194, we obtain a tight correlation in both HS and HIMS. This leads us to conclude that the jet could be compact throughout the outburst, though the possibility of fast and slow components cannot be ruled out. Russell et al. (2015) also reported on the compact nature of the jet for this BHC.

In the future, we would like to find disk-jet coupling for other BHCs. So far, we found $F_R \sim F_{\rm ouf}^{0.6}$ for MAXI J1836–194 and Swift J1753.5–0127. We would like to see if this relation holds in some other cases as well.

Acknowledgements A.J. and D.D. acknowledge support from DST/GITA sponsored by the India-Taiwan collaborative project fund (GITA/DST/TWN/P-76/2017). D.C. and D.D. acknowledge support from DST/SERB sponsored by the Extra Mural Research project (EMR/2016/003918). Research by D.D. and S.K.C. is supported in part by the Higher Education Dept. of the Govt. of West Bengal, India. D.D. also acknowledges support from the ISRO sponsored RESPOND project (ISRO/RES/2/418/17-18) fund. This research has made use of the XRT Data Analysis Software (XRTDAS) developed under the responsibility of the ASI Science Data Center (ASDC), Italy.

References

Aktar, R., Das, S., & Nandi, A. 2015, MNRAS, 453, 3414
Arnaud, K. A. 1996, ASP Conf. Ser., Astronomical Data Analysis Software and Systems V, eds. G. H. Jacoby, & J. Barnes, 101, 17
Bhattacharjee, A., Banerjee, I., Banerjee, A., et al. 2017, MNRAS, 466, 1372
Blandford, R. D., & Znajek, R. L. 1977, MNRAS, 179, 433
Blandford, R. D., & Payne, D. G. 1982, MNRAS, 199, 883
Blandford, R. D., & Begelman, M. C. 1999, MNRAS, 303, L1
Camenzind, M. 1989, ASSL, 156, 129
Chakrabarti, S. K. 1989, ApJ, 347, 365
Chakrabarti, S. K. 1990a, Theory of Transonic Astrophysical Flows (World Scientific: Singapore)
Chakrabarti, S. K. 1990b, MNRAS, 243, 610
Chakrabarti, S. K., & Bhaskaran, P. 1992, MNRAS, 255, 255
Chakrabarti, S. K. & Molteni, D. 1995, MNRAS, 272, 80
Chakrabarti, S. K., & Titarchuk, L. G. 1995, ApJ, 455, 623
Chakrabarti, S. K. 1996, ApJ, 464, 664
Chakrabarti, S. K. 1997, ApJ, 484, 313
Chakrabarti, S. K. 1999a, A&A, 351, 185 (C99a)
Chakrabarti, S. K. 1999b, Ind. J. Phys., 73, 6, 931 (C99b)
Chakrabarti, S. K., & Nandi, A. 2000, Ind. J. Phys., 75, 1 (arXiv:0012526)
Chakrabarti, S. K. 2001, AIPC, 558, 831 (arXiv:0012522)
Chakrabarti, S. K., Nandi, A., Manickam, S. G., et al. 2002, ApJ, 579, L21
Chakrabarti, S. K., & Das, S. 2004, MNRAS, 349, 649
Chatterjee, D., Debnath, D., Chakrabarti, S. K., et al. 2016, ApJ, 827, 88
Chatterjee, D., Debnath, D., Jana, A., & Chakrabarti, S. K. 2019a, Ap&SS, 364, 14
Chatterjee, D., Debnath, D., Jana, A., et al. 2019b, MNRAS (submitted)
Chattopadhyay, I., & Chakrabarti, S. K. 2000, IJMPD, 9, 57
Chattopadhyay, I., & Chakrabarti, S. K. 2001, AIPC, 558, 835
Chattopadhyay, I., & Chakrabarti, S. K. 2002, MNRAS, 333, 454
Chattopadhyay I., & Das S. 2007, New Astronomy, 12, 454
Corbel, S., Fender, R. P., Tzioumis, A. K., et al. 2000, A&A, 359, 251
Corbel, S., Nowak, M. A., Fender, R. P., et al. 2003, A&A, 400, 1007
Corbel, S., Tomsick, J. A., & Kaaret, P. 2006, ApJ, 636, 971
Corbel, S., Coriat, M., & Brocksopp, C. 2013, MNRAS, 428, 2500
Coriat, M., Corbel, S., Prat, L., et al. 2011, MNRAS, 414, 677
Das, T. K., & Chakrabarti, S. K. 1999, CQGra, 16, 3879
Debnath, D., Chakrabarti, S. K., & Nandi, A. 2010, A&A, 520, 98
Debnath, D., Mondal, S., & Chakrabarti, S. K. 2014, MNRAS, 440, L121
Debnath, D., Mondal, S., & Chakrabarti, S. K. 2015a, MNRAS, 447, 1984
Debnath, D., Molla, A. A., Chakrabarti, S. K., & Mondal, S. 2015b, ApJ, 803, 59
Debnath, D., Jana, A., Chakrabarti, S. K., & Chatterjee, D. 2017, ApJ, 850, 92
Fabrika S. 2004, Astrophysics and Space Physics Reviews, 12, 1
Falcke, H., & Biermann, P. L. 1995, A&A, 293, 665
Falcke, H., & Markoff, S. 2000, A&A, 362, 113
Fender, R. P., Belloni, T. M., & Gallo, E. 2004, MNRAS, 355, 1105
Ferrigno, C., Bozzo, E., Del, S., et al. 2012, A&A, 537, L7
Garain, S. K., Ghosh, H., & Chakrabarti, S. K. 2012, ApJ, 758, 114
Gallo, E., Fender, R. P., & Pooley, G. G. 2003, MNRAS, 344, 60
Gallo, E., Corbel, S., Fender, R. P., Maccarone, T. J., & Tzioumis, A. K. 2004, MNRAS, 347, L52

Gallo, E., Fender, R. P., Miller-Jones, J. C. A., et al. 2006, MNRAS, 370, 1351
Gallo, E., Miller-Jones, J. C. A., Russell, D. M., et al. 2014, MNRAS, 445, 290
Grebenev, S. A., Prosvetov, A. V., & Sunyaev, R. A. 2013, AstL, 39, 367
Hannikainen, D. C., Hunstead, R. W., Campbell Wilson, D., & Sood, R. K. 1998, A&A, 337, 460
Heinz, S., & Sunyaev, R. A. 2003, MNRAS, 343, L59
Heinz, S. 2004, MNRAS, 355, 835
Jana, A., Debnath, D., Chakrabarti, S. K., et al. 2016, ApJ, 819, 107 (Paper-I)
Jana, A., Chakrabarti, S. K., & Debnath, D. 2017, ApJ, 850, 91 (JCD17)
Jonker, P. G., Miller-Jones, J., Homan, J., et al. 2010, MNRAS, 401, 1255
Jonker, P. G., Miller-Jones, J. C. A., Homan, J., et al. 2012, MNRAS, 423, 3308
Krimm, H. A., Barthelmy, S. D., Baumgartner, W., et al. 2012, Atel, 3966, 1
Kording, E., Falcke, H., & Corbel, S. 2006, A&A, 456, 439
Markoff, S., Falcke, H., & Fender, R. 2001, A&A, 372, L25
Markoff, S., Nowak, M., Corbel, S., et al. 2003, A&A, 397, 645
Merloni, A., Heinz, S., & di Matteo, T. 2003, MNRAS, 345, 1057
Mirabel, I. F., Rodríguez, L. F., Cordier, B., Paul, J., & Lebrun, F. 1992, Nature, 358, 215
Mirabel, I. F., & Rodríguez, L. F. 1994, Nature, 371, 46
Molla, A. A., Debnath, D., Chakrabarti, S. K. et al. 2016, MNRAS, 460. 3163
Molla, A. A., Debnath, D., Chakrabarti, S. K. et al. 2017, ApJ, 834, 88
Mondal, S., Debnath, D., & Chakrabarti, S. K. 2014, ApJ, 786, 4
Mondal, S., Chakrabarti, S.K., & Debnath, D. 2016, Ap&SS, 361, 309
Narayan, R., Igumenshchev, I. V., & Abramowicz, M. A. 2003, PASJ, 55, L69
Negoro, H., Nakajima, M., Nakahira, S., et al. 2011, ATel, 3611, 1
Plotkin, R. M., Gallo, E., & Jonker, P. G. 2013, ApJ, 773, 59
Plotkin, R. M., Miller-Jones, J. C. A., & Gallo, E. 2017, ApJ, 834, 104
Ratti, E. M., Jonker, P. G., Miller-Jones, J. C. A., et al. 2012, MNRAS, 423, 2656
Reis R. C., Miller, J. M., Reynolds, M. T., et al. 2012, ApJ, 751, 34
Remillard R., & McClintock, J. 2006, ARA&A, 44, 49
Rodríguez, L. F., Mirabel, I. F., & Marti, J. 1992, ApJ, 401, L15
Rushton, A. P., Shaw, A. W., Fender, R. P., et al. 2016, MNRAS, 463, 628
Russell, D. M., Russell, T. D., Miller-Jones, J. C. A., et al. 2013, ApJ, 768, 35
Russell, T. D., Soria, R., Motch, C., et al. 2014a, MNRAS, 439, 1381
Russell, T. D., Soria, R., Miller-Jones, J. C. A., et al. 2014b, MNRAS, 439, 1390
Russell, T. D., Miller-Jones, J. C. A., & Curran, P. A. 2015, MNRAS, 450, 1745
Shakura, N. I., & Sunyaev, R. A. 1973, A&A, 24, 337
Shang, J.-R., Debnath, D., Chatterjee, D., et al. 2019, ApJ, 875, 4
Soleri, P., Fender, R. P., Tudose, V., et al. 2010, MNRAS, 406, 1471
Stirling, A. M., Spencer, R. E., de la Force, C. J., et al. 2001, MNRAS, 327, 1273
Sunyaev, R.A., & Titarchuk, L. G. 1980, ApJ, 86, 121
Sunyaev, R.A., & Titarchuk, L. G. 1985, A&A, 143, 374
Yang, Y. J., Wijnands, R., & Kennea, J. A. 2012a, ATel, 3975, 1
Yang, J., Xu, Y., & Li, Z. 2012b, MNRAS, 426, 66